CHEMISTRY
A European Journal

A Journal of
ChemPubSoc Europe

Accepted Article

Title: Iron Porphyrin Does Fast and Selective Electrocatalytic Conversion of CO2 to CO in a Flow Cell

Authors: Kristian Torbensen, Cheng Han, Benjamin Boudy, Niklas von Wolff, Caroline Bertail, Waldemar Braun, and Marc Robert

To be cited as: *Chem. Eur. J.* 10.1002/chem.202000160

Link to VoR: http://dx.doi.org/10.1002/chem.202000160

Supported by
ACES

WILEY-VCH

10.1002/chem.202000160

WILEY-VCH

COMMUNICATION

Iron Porphyrin Does Fast and Selective Electrocatalytic Conversion of CO_2 to CO in a Flow Cell

Kristian Torbensen,[a] Cheng Han,[a],[b] Benjamin Boudy,[a] Niklas von Wolff,[a] Caroline Bertail,[c] Waldemar Braun[d] and Marc Robert*[a]

Abstract: Molecular catalysts have been shown to have high selectivity for CO_2 electrochemical reduction to CO, but with current densities significantly below those obtained with solid-state materials. By depositing a simple Fe porphyrin mixed with carbon black onto a carbon paper support, we have obtained a catalytic material that could be used in a flow cell for fast and selective conversion of CO_2 to CO. At neutral pH (7.3) a current density as high as 83.7 mA cm^{-2} was obtained with a CO selectivity close to 98%. In basic solution (pH 14), a current density of 27 mA cm^{-2} was maintained for 24 h with 99.7% selectivity for CO at only 50 mV overpotential, leading to a record energy efficiency of 71%. In addition, a current density for CO production as high as 152 mA cm^{-2} (>98% selectivity) was obtained at a low overpotential of 470 mV, outperforming state-of-the-art noble metal based catalysts.

CO_2 may be used as renewable feedstock for producing fuels or commodity chemicals with renewable electricity as energy source.[1-2] However, selective, robust and fast electrochemically driven conversion of CO_2 remains a great challenge in the scientific field and as well as in the industrial environment. Therefore, new approaches are needed to develop electrolyzers operating at industrial relevant scales while fulfilling customer needs and requirements. Regarding the catalysts employed, molecular complexes have been widely investigated for the carbon dioxide reduction reaction (CO_2RR) due to the possibility of fine tuning the ligand structure (steric and electronic effects, as well as second coordination sphere effects).[3-6] Earth abundant metal-based catalysts have been shown to efficiently catalyze the production of CO and formate in organic solvents and in water,[7-11] even if examples in pure aqueous solutions are less numerous. In the latter case, the catalysts are typically dispersed into thin conductive films usually made of carbon nanomaterials, such as carbon black or carbon nanotubes.[12-20] Until very recently, these molecular catalysts were deemed to be incapable to operate in flow cells at both high product selectivity and conversion rate. Using Co phthalocyanine as catalysts, we have shown that this dogma can be overcome by applying the complex into a flow cell, generating CO with 94% selectivity at 165 mA/cm^2 current density at basic pH (14).[21-22] Such performances approach those obtained with Ag and Au based catalytic materials.[23-25] However, the Co complex, like the above mentioned solid nano-catalysts, operates at quite large overpotential, in the range of 800 mV at comparably current densities. The selectivity could also be still improved, while the exclusive use of earth abundant elements instead of expensive metals is mandatory. In this context, Fe is an ideal candidate being the most abundant transition metal. As previously shown, tetraphenyl Fe porphyrin substituted with trimethyl ammonium groups at the para position of each of the four phenyl groups (**FeP**, Scheme 1 (left),[26-27] is able to produce CO with a selectivity of 90% at neutral pH and at an overpotential of 450 mV. However, maximum current density obtained in an H-cell device was in the range of 1 mA cm^{-2}.[27] Using **FeP**/graphene framework[28] or **FeP**/graphene hydrogel[29] assemblies also led to high selectivity for CO (96-98.7%) and a maximum current density of about 1.7 mA cm^{-2} at ca. 430 mV overpotential was shown. Supramolecular porous structures made of Fe tetraphenylporphyrin units have also been used as catalysts.[30-31] After deposition at the surface of a carbon electrode, it led to good selectivity for CO production (ca. 90%), with a current density of 1.2 mA cm^{-2} at ~ 500 mV overpotential. With these encouraging preliminary results at hand, and keeping in mind the idea of a simple, cheap and easy-to-prepare material, we manufactured gas diffusion electrodes by depositing a thin nanoscaled film containing **FeP** and carbon particles onto a carbon paper support. When implemented in an electrolyzer, this catalytic material proved to be exceptionally active for the CO_2RR, even surpassing the performance of noble metal based nanomaterials.

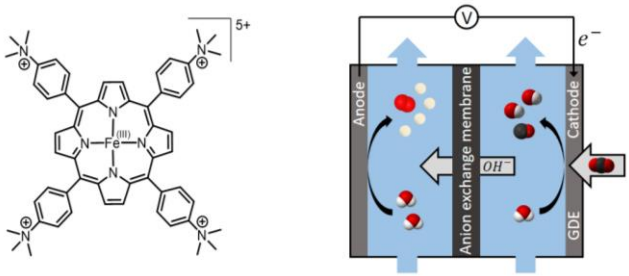

Scheme 1. Structure of the catalyst **FeP** (left, counterions omitted for clarity) and schematic view of the flow cell operating in pH neutral conditions (right).

The catalytic ink was prepared from a suspension of carbon black and **FeP**. It allows to ensure good electronic conduction between the molecular catalyst and the support. The ink was deposited onto carbon paper by drop casting, leading to a 1 cm^2 gas diffusion electrode (GDE), with a **FeP** loading of 2.08 mg cm^{-2}. SEM images of the film are shown in Figure S1. Qualitative EDX elemental mapping analysis was performed and a homogeneous

[a] Dr., K., Torbensen, Dr., C., Han, Mr. B., Boudy, Dr., N., von Wolff, Prof., Dr. M., Robert
Université de Paris, Laboratoire d'Electrochimie Moléculaire, CNRS, F-75013 Paris, France
E-mail: robert@univ-paris-diderot.fr
[b] Dr., C., Han
College of Aerospace Science and Engineering, National University of Defense Technology, 109 Deya Road, Changsha, Hunan 410073, P. R. China
[c] Dr. C., Bertail,
Air Liquide Research&Development Paris Innovation Campus, F-78354 Jouy en Josas, France
[d] Dr. W., Braun
Air Liquide Forschung und Entwicklung GmbH, Gwinnerstraße 27-33, 60388 Frankfurt, Germany

Supporting information for this article is given via a link at the end of the document.

10.1002/chem.202000160

distribution of the catalyst at the GDE (Figure S2) was found. We then verified that immobilization of the catalyst did not alter its molecular integrity. Fe K-edge X-Ray absorption near-edge structure spectra recorded at a **FeP** loaded GDE and from a **FeP** pellet did not show any significant difference (Figure S3A), while UV-vis spectra of **FeP** was similar to the spectra obtained after extracting the complex from a GDE using DMF as solvent (Figure S3B). Cyclic voltammetry was also performed at a GDE to verify that the **FeP** was electrochemically active. However, due to the hydrophobic nature of the film, only a small fraction of the total amount of catalyst could be addressed when interrogated from the front side of the GDE (see Figure S4 for further explanation). Upon introducing CO_2 to the electrochemical cell, a clear catalytic response was observed (Figure S5). The catalyst coated GDE was then inserted into a flow cell setup, Scheme 1 (right). The electrolyzer consists of a sandwich of mounted flow frames, electrodes, gaskets and an ion exchange membrane, which were assembled as schematically illustrated in Figure S6. CO_2 is allowed to flow *through* the gas diffusion electrode, while the catholyte solution is circulated in between the GDE and the anion exchange membrane (AEM). Within the GDE, CO_2 undergoes a 2-electron-2-proton reduction forming CO and OH^-. In the anodic compartment, water is oxidized to dioxygen and H^+ at a Pt/Ti alloy electrode. The AEM allows for diffusion of OH^-, thereby maintaining overall electroneutrality upon reacting with protons. In the following electrolysis experiments, no liquid CO_2 reduction products could be detected by NMR or ion chromatography.

Catalytic activity was first investigated as a function of the applied potential in a CO_2-saturated 0.5 M $NaHCO_3$ solution. Figure 1 illustrates the current density increase as a function of the potential, along with the selectivity for CO production (see also Table S1). At a low overpotential (η) of 270 mV (no IR drop correction was applied throughout the paper), CO was detected as the only product (99.9% selectivity) with a total current density of 7.2 mA cm^{-2}. Selectivity for carbon monoxide remained above or equal to 99% up to 700 mV overpotential, and H_2 was the only minor by-product that could be detected. At a potential of -0.98 V vs. RHE, the current density reached 42.1 mA cm^{-2} along with 98.6% CO selectivity. The catalyst ability to suppress the H_2 evolution reaction (HER) in favor of the CO_2RR was further verified by inserting in the electrolyzer a carbon film with non-metalated porphyrin, which resulted in exclusive H_2 production (Figure S7).

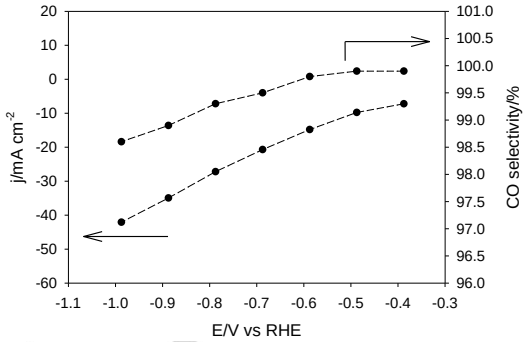

Figure 1. Current density (left axis) at the gas diffusion electrode and CO selectivity (right axis) as a function of the applied potential in 0.5 M $NaHCO_3$ electrolyte solution.

The endurance of the catalytic film was tested by performing a 24 h chronoamperometric electrolysis at -0.78 V vs RHE, so as to compromise between high rate and selectivity. As shown in Figure 2, excellent stability was obtained during the whole course of the electrolysis, with an average current density of 27.3 mA cm^{-2} and 98.2 ± 0.2% selectivity for CO. It corresponds to a production of 0.5 mmol h^{-1} CO, which, based on the total catalyst loading (1.37 µmol cm^{-2}), gives a lower limit for the TON of 8765 and TOF of 365 h^{-1}. The TON and TOF values reported herein are thus significantly underestimated. The cell potential (E_{cell}) was 3.4 V and an energy efficiency (EE) of 39% was calculated from EE = FE% x $\Delta E^0/E_{cell}$, where ΔE^0 is the apparent standard potential difference between the anodic and cathodic reactions (1.34 V). EDX elemental mapping analysis was performed at the **FeP** loaded GDE after the 24 h electrolysis, showing almost no change in elemental composition and no aggregation of iron, which remains homogeneously dispersed in the film (Figure S8). XANES of the GDE and UV-vis of catalyst extracted from the GDE after electrolysis further proved the molecular integrity of **FeP** intact (Figures S9A and S9B).

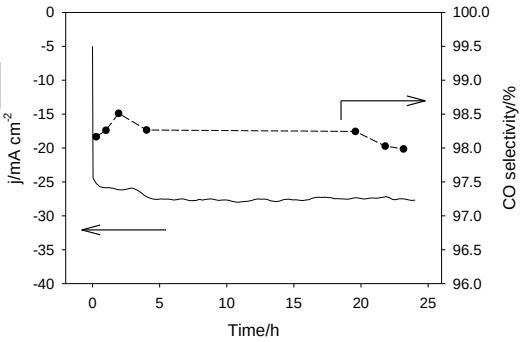

Figure 2. Current density (left axis) and CO selectivity (right axis) during a 24 h electrolysis at E = -0.78 V vs RHE in 0.5 M $NaHCO_3$ electrolyte solution.

Encouraged by these results, a high current density of 50 mA cm^{-2} could be sustained for about 3 hours at a potential of -1.14 V vs RHE (η = 1.03 V), with 98.3 ± 0.3% average selectivity and a production of 0.9 mmol h^{-1} CO (Figure S10). This was obtained at the expense of an increase of the cell potential (4.05 V), lowering the EE to 33%. The Ohmic resistance of the electrolyzer cell could be reduced upon increasing the electrolyte concentration. Using a 1.0 M $NaHCO_3$ electrolyte solution, a current density of 50 mA cm^{-2} was sustained for 3 h at only -0.86 V vs RHE (η = 0.75 V), reducing the cell potential by 590 mV and increasing the energy efficiency up to 38% (Figure S11). The CO product selectivity was maintained at a high value of 99.0 ± 0.2% on average. Increasing the temperature from 24 °C up to 40 °C led to larger current densities, as shown in Figure 3, while maintaining a high CO selectivity. At E = -0.78 V vs RHE, the current density raised from 28 to 39 mA cm^{-2} (in 0.5 M $NaHCO_3$). It was verified that the pH of the electrolyte solution was about constant within this temperature range. Regarding thermodynamics, increasing the temperature amounts to decreasing the overpotential since the

10.1002/chem.202000160

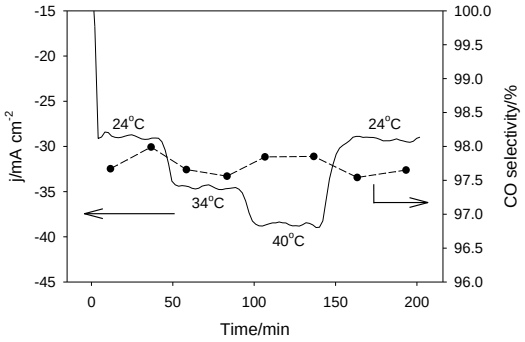

Figure 3. Current density (left axis) and CO selectivity (right axis) obtained at various temperatures as indicated. Electrolysis performed at E = -0.78 V vs RHE in 0.5 M $NaHCO_3$ electrolyte solution.

apparent standard potential for converting CO_2 into CO is E^0 – (RT ln10/2F) x pH. Thus, the observed rate increase could be attributed to enhanced kinetics.

As recently demonstrated,[32] the GDE likely counter-balances CO_2 solubility decrease when T is raised, preventing catalysis limitation by mass transport and ensuring a constant (steady state) CO_2 concentration at the catalytic sites. TOF values are hence equivalent to pseudo first order rate constant for the CO production. An Eyring plot provided an activation enthalpy of 9.5 kJ mol^{-1} and an activation entropy of -231 $Jmol^{-1}$ K^{-1}, suggesting an associative rate determining step, possibly CO_2 binding to the reduced **FeP**, as already proposed from electrochemical studies (Figure S12). A prolonged electrolysis was performed for 3 h at a constant current density of 50 mA cm^{-2} (in 0.5 M $NaHCO_3$) at 40° C (Figure S13), leading to 98.6 ± 0.1% selectivity for CO at an average overpotential of just 730 mV (compared to 1.03 V at 24° C), illustrating the positive impact of such small temperature increase.

Besides increasing the electrolyte salt concentration and temperature, it was recently shown that the cation size of the electrolyte may also impact the catalytic performance.[33-34] Using a 0.5 M $CsHCO_3$ as electrolyte solution (see Figure S14 and Table S2), a significant performance increase was obtained with a current density of 9 mA cm^{-2} at 270 mV overpotential (99.9% CO selectivity) and a current density (at η = 870) of 83.7 mA cm^{-2} (97.6% selectivity), a value two times larger than the one obtained using a 0.5 M $NaHCO_3$ solution. Comparative electrolysis at 50 mA cm^{-2} (Figure S15) led to a 390 mV overpotential decrease along with a slight CO selectivity increase and an EE gain of 8%, as summarized in Table 1. As recently suggested by Chan et al.,[34] cations having the smallest hydration radius, which is inversely proportional to the ionic radius, may lead to the strongest interfacial electric field, favoring CO_2 adsorption at catalytic sites.

Table **1.** Catalytic performances for 3h electrolysis at 50 mA cm^{-2} in a 0.5 M electrolyte solution ($NaHCO_3$, $KHCO_3$ or $CsHCO_3$).

Cation	E/V vs RHE	η/V	CO Selectivity/%	EE/%
Na^+	-1.14	1.03	98.3	33
K^{+*}	-0.95	0.84	98.6	36
Cs^+	-0.75	0.64	98.9	41

*Electrolysis in 0.5 M $KHCO_3$ electrolyte (Figure S16) was performed so as to confirm the trend described in the text.

Alkaline conditions allowed to boost the performance a step further. Using 1 M KOH as electrolyte, a current density of 37.6 mA cm^{-2} was obtained at 70 mV overpotential with perfect selectivity for CO (99.9%). A current density of 155 m Acm^{-2} was reached at η = 470 mV with a selectivity for CO of 98.1%, corresponding to a partial current density for CO (j_{CO}) of 152 mA cm^{-2} (see Figure 4 and Table S3). Such current density for CO production is significantly higher than that obtained with a state-of-the art noble metal based material (500 nm thick Ag film mixed with carbon particles and deposited at a PTFE membrane) which gave a j_{CO} of ca. 90 mA cm^{-2} at η ~ 480 mV.[24] Figure 4 display the current density increase as a function of the potential, along with the selectivity for CO production (see also Table S3). A control experiment with the non-metalated porphyrin ligand only afforded H_2 as reduction product (Figure S17).

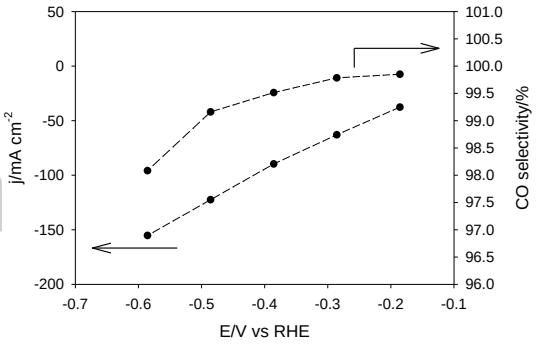

Figure 4. Current density (left axis) at the gas diffusion electrode and CO selectivity (right axis) as a function of the applied potential in 1 M KOH electrolyte solution.

To compare the endurance of **FeP** in similar conditions with the pervious results gathered at pH close to neutral, a chronopotentiometric electrolysis was performed at 27 mA cm^{-2} for 24 h. As shown in Figure 5, an average potential of -0.16 V vs RHE (η = 0.05 V) was measured, showing only a minute increase over time. The CO product selectivity was 99.7 ± 0.2% on average with a total CO production of 0.5 mmol h^{-1}, a TON of 8719 and a

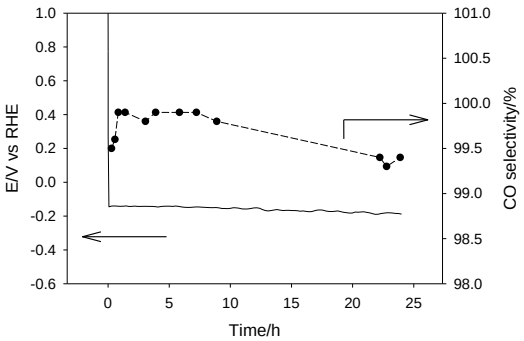

Figure 5. Applied potential (left axis) and CO selectivity (right axis) for a 24 h electrolysis performed at 27 mA cm^{-2} in 1 M KOH electrolyte solution.

TOF of 363 h^{-1}. The cell potential was only 1.87 V, corresponding to an EE of 71%. EDX elemental mapping of the GDE after the 24 h electrolysis showed that **FeP** was still present and homogeneously dispersed in the film (Figure S18). XANES of the GDE and UV-vis of catalyst extracted from the GDE after electrolysis further proved the molecular integrity of **FeP** intact (Figures S19A and S19B). Finally, at 50 mA cm^{-2} current density, a remarkably low overpotential of 120 mV was maintained during a 3 h electrolysis, producing 0.9 mmol h^{-1} CO with 99.8 ± 0.2% selectivity, a TON of 2023 and a TOF of 674 h^{-1}, along with an EE of 57% (Figure S20).

In conclusion, **FeP** appears as an exceptionally efficient supported homogeneous catalyst for the conversion of CO_2 to CO in water once inserted in a flow cell. From neutral pH to alkaline conditions, selectivities larger than 98% were systematically obtained, thanks to the high reactivity of the catalyst with CO_2 and the low overpotential values that makes the HER pathway unfavorable. The catalytic material proved to be stable under operating conditions over prolonged electrolysis time. Slight increase in temperature (from 25 to 40 °C) as well as increasing the electrolyte concentration and the cation size were beneficial to both the CO production rate, the selectivity of the CO_2-to-CO conversion and the energy efficiency. Remarkably, a very high current density for CO could be obtained at a low overpotential (j_{CO} > 150 mA cm^{-2} at η = 470 mV), outperforming state of the art silver based nanomaterials. These results illustrate that molecular catalysts can be used in flow cell devices and are candidates for being included into large scale CO_2 electrolyzers.

Acknowledgements

The work described in this project was financed in part by Air Liquide and the *Institut Universitaire de France* (IUF). PhD fellowship to C. H from China Scholarship Council (CSC, grant number 201603170259) is gratefully acknowledged. We thank Ms. D. Mendoza and Dr. B. Lassalle-Kaiser for collecting Xray absorption data at SOLEIL synchrotron facilities.

Keywords: • carbon dioxide reduction • carbon monoxide • Fe complex • flow cell • hybrid materials •

[1] A. Tatin, J. Bonin, M. Robert, *ACS Energy Lett.* **2016**, *1*, 1062-1064.
[2] P. De Luna, C. Hahn, D. Higgins, S. A. Jaffer, T. F. Jaramillo, E. H. Sargent, *Science* **2019**, *364*, eaav3506.
[3] H. Takeda, C. Cometto, O. Ishitani, M. Robert, *ACS Catal.* **2017**, *7*, 70-88.
[4] K. A. Grice, *Coord. Chem. Rev.* **2017**, 336, 78-95.
[5] R. Francke, B. Schille, M. Roemelt, *Chem. Rev.* **2018**, 118, 4631-4701.
[6] K. E. Dalle, J. Warnan, J. J. Leung, B. Reuillard, I. S. Karmel, E. Reisner, *Chem. Rev.* **2019**, 119, 2752-2875.
[7] N. D. Loewen, T. V. Neelakantan, L. A. Berben, *Acc. Chem. Res.* **2017**, 50, 2362-2370.
[8] C. Costentin, M. Robert, J-M. Savéant, A. Tatin, *Proc. Natl. Acad. Sci. USA* **2015**, 112, 6882-6886.
[9] I. Azcarate, C. Costentin, M. Robert, J.-M. Savéant, *J. Am. Chem. Soc.* **2016**, 138, 16639-16644.
[10] N. D. Loewen, T. V. Neelakantan, L. A. Berben, *Acc. Chem. Res.* **2017**, 50, 2362-2370.
[11] E. A. Mohamed, Z. N. Zahran, Y. Naruta, *Chem. Mat.* **2017**, 29, 7140-7150.
[12] S. Aoi, K. Mase, K. Ohkubo, S. Fukuzumi, *Chem. Commun.* **2015**, 50, 10226-10228.
[13] A. Maurin, M. Robert, *J. Am. Chem. Soc.* **2016**, 138, 2492-2495.
[14] X-M. Hu, M. H. Ronne, S. U. Pedersen, T. Skrydstrup, K. Daasbjerg, *Angew. Chem. Int. Ed.* **2017**, 56, 6468-6472.
[15] X. Zhang, Z. Wu, X Zhang et al., *Nat. Commun.* **2017**, 8:14675.
[16] N. Han, Y. Wang, L. Ma et al., *Chem* **2017**, 3, 652-664.
[17] M. Wang, L. Chen, T-C. Lau, M. Robert, *Angew. Chem. Int. Ed.* **2018**, 57, 7769-7773.
[18] J. Choi, P. Wagner, S. Gambir, R. Jalili, D. R. MacFarlane, G. G. Wallace, D. L. Officer, *ACS Energy Lett.* **2019**, 4, 666-672.
[19] M. Zhu, J. Chen, L. Huang, R. Ye, J. Xu, Y-F. Han, *Angew. Chem. Int. Ed.* **2019**, 58, 6595-6599.
[20] L. Rotundo, J. Filippi, R. Rocca, R. Gobetto, H. A. Miller, C. Nervi, F. Vizza, *Chem. Commun.* **2019**, 55, 775-777.
[21] M. Wang, K. Torbensen, D. Salvatore, S. Ren, D. Joulie, F. Dumoulin, D. Mendoza, B. Lassalle-Kaiser, U. Işci, C. Berlinguette, M. Robert, *Nat. Commun.* **2019**, 10:3602.
[22] S. Ren, D. Joulie, D. Salvatore, K. Torbensen, M. Wang, M. Robert, C. Berlinguette, *Science* **2019**, 365, 367-369.
[23] R. B. Kutz, Q. Chen, H. Yang, S. D. Sajjad, Z. Liu, I. R. Masel, *Energy Technol.* **2017**, 5, 929-936.
[24] C-T., Dinh, F. P., García de Arquer, D. Sinton, D., E. H. Sargent, *ACS Energy Lett.* **2018**, 3, 2835−2840.
[25] S. Verma, Y. Hamasaki, C. Kim, W. Huang, S. Lu, S., H-R. M., Jhong, A. A. Gewirth, T. Fujigaya, N. Nakashima, P. J. A. Kenis, *ACS Energy Lett.* **2018**, 3, 193−198.
[26] C. Costentin, M. Robert, J-M. Savéant, A. Tatin, *Proc. Natl. Acad. Sci. USA* **2015**, 112, 6882-6886.
[27] A. Tatin, C. Cominges, B. Kokoh, C. Costentin, M. Robert, J-M. Savéant, *Proc. Natl. Acad. Sci. USA* **2016**, 113, 5526-5529.
[28] J. Choi, P. Wagner, S. Gambir, R. Jalili, J. Kim, D. R. MacFarlane, G. G. Wallace, D. L. Officer, *Adv. Energy Mater.* **2018**, 1801280.
[29] J. Choi, J. Kim, P. Wagner, S. Gambir, R. Jalili, S. Byun, S. Sayyar, Y. M. Lee, D. R. MacFarlane, G. G. Wallace, D. L. Officer, *Energy Environ. Sci.* **2019**, 12, 747-755.
[30] P. T. Smith, B. P. Benke, Z. Cao, Y. Kim, E. M. Nichols, K. Kim, C. J. Chang, *Angew. Chem. Int. Ed.* **2018**, 57, 9684-9688.
[31] B-X. Dong, S-L. Qian, F-Y. Bu, Y-C. Wu, L-G. Feng, Y-L. Teng, W-L. Liu, Z-W Li, *ACS Appl. Energy Mater.* **2018**, 1, 4662-4669.
[32] A. Löwe, C. Rieg, T. Hierlemann, N. Salas, D. Kopjlar, N. Wagner, E. Klemm, *ChemElectroChem* **2019**, 6, 4497-4506.
[33] M. M. de Salles Pupo, R. Kortlever, *ChemPhysChem*, doi.org/10.1002/cphc.201900680.
[34] S. Ringe, E. L. Clark, J. Resasco, A. Walton, B. Seger, A. T. Bell, K. Chan, *Energy Environ. Sci.* **2019**,12, 3001-3014.

10.1002/chem.202000160

WILEY-VCH

Entry for the Table of Contents (Please choose one layout)

Layout 1:

COMMUNICATION

Text for Table of Contents

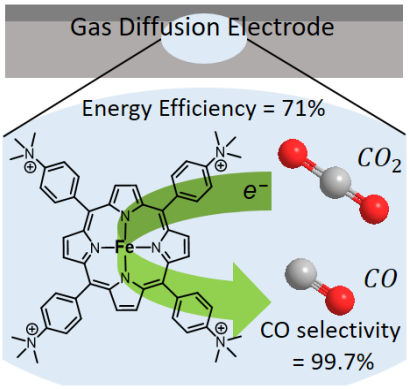

*Kristian Torbensen, Cheng Han, Benjamin Boudy, Niklas von Wolff, Caroline Bertail, Waldemar Braun and Marc Robert**

Page No. – Page No.

Iron Porphyrin Does Fast and Selective Electrocatalytic Conversion of CO_2 to CO in a Flow Cell